13.4 Observation-Based Wind-Power Ramp Forecast System

Seth Linden*, Bill Myers, Sue Ellen Haupt
National Center for Atmospheric Research
Boulder, CO

1. INTRODUCTION

Over the last several years wind-energy production has increased world-wide. Wind-energy is now becoming a viable and integral part of the new energy economy. As wind energy becomes increasingly more prevalent, having accurate wind-power forecasts becomes important in order to help energy operators make better grid integration and economic decisions. Since a majority of energy trading is done 24 hours in advance, most of the wind-power forecasts that are utilized by operators today are aimed at reducing the uncertainty in wind-power production 24-48 hours in advance. Although this is an important component, these forecasts do not address short-term issues such as sudden wind-power ramps.

Unforeseen wind-power ramps caused by a sudden increase in wind-speed over a wind plant can produce excess energy that cannot be used because energy has already been allocated from other sources. If operators have some indication that a wind ramp is approaching in the next few hours, they can shut down other sources of energy in order to fully utilize the wind-power produced by the wind power amp. Therefore, short-term forecasts (0-6 hours out) specifically designed to forecast wind ramps are becoming increasingly more important.

* *Corresponding author address*: Seth Linden, National Center for Atmospheric Research, Research Applications Laboratory (RAL), Boulder, CO, 80301; e-mail: linden@ucar.edu

In conjunction with the Xcel Energy wind-power forecasting project at NCAR, research and development efforts have been performed to determine if publicly available upstream observations could be used to predict when a ramp is likely to impact a wind farm. This paper discusses an experimental observation-based wind ramp forecasting expert system configured at NCAR for one of the Xcel wind farms. The techniques used to utilize upstream surface observations to predict wind-power ramps at the farm are laid out. The algorithm's performance is examined for a number of cases. A summary of the algorithm's strengths and weaknesses is discussed. Lastly, recommendations are made about future work.

2. BACKGROUND

In 2008 NCAR was tasked with researching and developing a wind-power forecast system for Xcel Energy. Xcel is for a utility that provides energy in three distinct regions of the US, which are roughly described as Minnesota, Colorado, and North Texas/East New Mexico. In these three regions, there is roughly 3.7 GW of installed wind power capacity from over 3000 wind turbines (Myers et al. 2011). With this much capacity, decisions made about how much power production will come from the wind versus other sources can have big economic impacts. Therefore it became apparent to Xcel that having a more accurate forecast that reduces the uncertainty in expected wind-power production, would save a substantial amount of money.

The Xcel wind-power forecast system is based on existing NCAR technologies, including the Dynamic Integrated ForeCast system (DICast). The DICast concepts were applied to making tuned hub-height wind-speed forecasts and then converting the predicted wind speeds to power. DICast is a weather prediction system that was designed to emulate the human forecast process. It first post-processes output of several individual NWP models separately, and then generates an intelligent consensus forecast from these optimized modules. A strength of DICast is that it continually learns how to make a better forecast based on comparisons of recent forecasts and observations (Myers et al. 2011). In this case it uses Nacelle wind-speed observations at the turbine hub to tune the wind-speed forecasts at hub-height. Other important components of the Xcel system include NCAR's high-resolution Weather Research and Forecasting (WRF) model, WRF-Ensemble and MM5-ensmble forecasts which are integrated into DICast along with the other publicly available NWP models and the use of a customized wind-speed-to-power conversion system.

The consensus averaging techniques employed in the system have proven to substantially reduce the day-ahead wind-power errors, and since this was the primary goal, the project has been considered successful with Xcel now using it operationally. Although the model consensus reduces wind-power error, it washes out temporal and spatial details and therefore lacks skill predicting sharp wind-ramps associated with smaller, distinct synoptic-scale and meso-scale features. It usually does well predicting ramps for well advertised large synoptic-scale events but typically is off with the timing. Forecasting wind-power ramps at a specific location and time is a very challenging problem. Currently, most approaches rely on high-resolution models such as the Weather Research and Forecasting (WRF) model to address this issue. High resolution modeling has shown some success at forecasting ramps, but often features are misplaced in time and space. Therefore other techniques, such as an observation-based system may be needed to better forecast wind ramps.

3. ALGORITHM CONCEPTS

The goal of the application is to see if nearby observation data can be used to predict when a wind ramp (or strong wind event) will occur at a wind farm within a 1-hour time window out to 6 hours in the future. The algorithm uses publicly available observing sites (METARs and mesonet sites) and searches for wind ramp signatures in upstream observations. Due to time constraints and funding limitations, the algorithm was only configured to predict ramps at a single wind farm in northeastern Colorado and only for features that originate from the north, northwest and northeast of the farm (currently only uses sites to the north of the farm). Figure 1 shows the observing sites that were used and their location relative to the farm (indicated by the red circle).

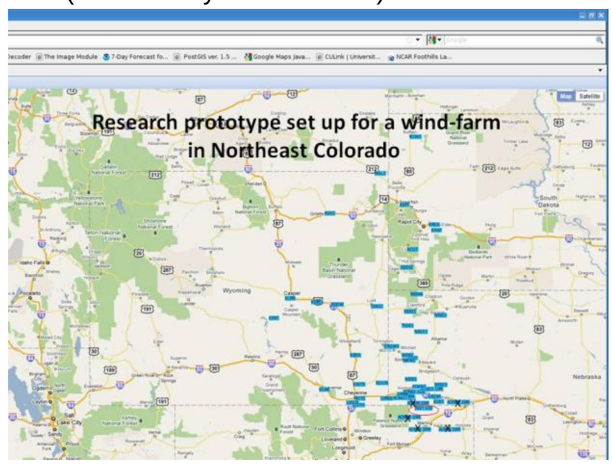

Figure 1. Map showing observing site locations relative to farm

First, observing sites are grouped together in rings based on their distance from the farm. The concept is that each ring of sites represents information that would impact the farm at different times; i.e. the closest ring of sites represents weather that could impact the farm in roughly 1 hour, the next ring out represents weather that could impact the farm in 2 hours and so on. In order to come up with the appropriate spacing for the rings this requires an assumption about how fast a wind feature will move from one location to another location downstream. After testing with different distances, 50 km spacing gave the best results. Although this may seem to imply rather fast movement of the weather systems, the verification results show that the algorithm is equally sometimes too early and sometimes too late with the ramp start.

The algorithm uses 8 groups of sites, represented by rings from the farm: 0-50km, 50-100km, 100-150km, 150-200km, ect. See Figure 2 for a schematic diagram of the setup. Since each ring of sites represents weather information that could impact the farm at different hours, the 1-hour lead-time forecast uses information from rings 1-8. The 2-hour lead-time forecast uses information from rings 2-8 (the first ring only represents weather that is 1 hour away). The 3-hour lead-time forecast uses rings 3-8 and so on. The shorter lead-time forecasts have more information to work with. Originally only 6 rings were used but that only allowed 2 rings of information for the 5-hour forecast and 1 ring of information for the 6 hour forecast. The number of rings were expanded to 8 in order to provided better information (more rings of sites) for the 4, 5 and 6 hour lead-time forecasts.

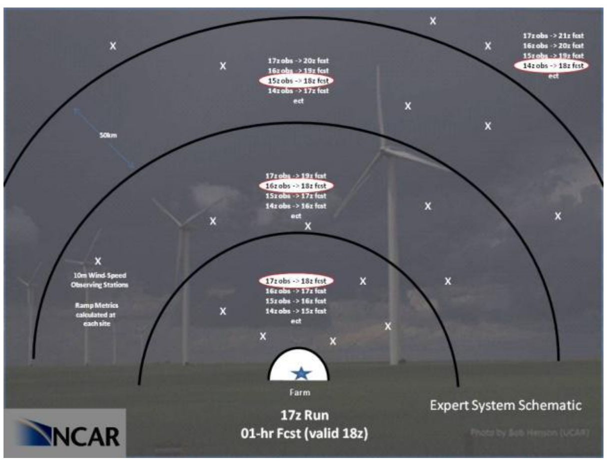

Figure 2. Schematic diagram of groups of sites separated by distance rings

For each site, and each historical hour, a ramp metric is calculated using the current hour and the previous hour 10 meter wind-speed observations. 10 meter wind-speed observations are converted to 80 meter estimates using a multiplier of 1.36 (this was determined from examining several equations that extrapolate surface wind to wind aloft). NCAR's wind-power class and ramp function is used to come up with a hub-height ramp metric using the pseudo 80 meter values. A history of observations (ramp metrics) is used in order to resolve all lead times. For example, the 1-hour lead-time forecast from the 17z run, valid at 18z, uses 17z ramp metrics from ring 1 (represents 1 hour away), the 16z ramp metrics from ring 2 (represents 2 hours away), the 15z ramp metrics from ring 3 (represents 3 hours away) and so on; as illustrated in Figure 2. The 2-hour lead time forecast from the 17z run, valid at 19z, does not use any ramp metrics from ring 1, the 17z ramp metrics from ring 2, the 16z metrics from ring 3, and so on; (see Figure 3).

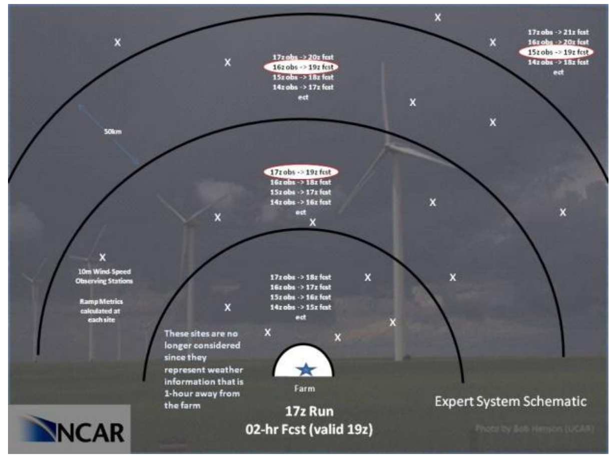

Figure 3. Schematic diagram showing what is used for the 2-hr lead time forecast

Once ramp metrics have been obtained for each site, the percentage of sites that are ramping (ramp metric > 0.25) are calculated in each group for each historical time. For a given lead time, the algorithm sums up the relevant group ramp percentages and calculates the average across all groups. Finally, it determines if a ramp is expected by thresh-holding the percentage of sites that are ramping across relevant groups and times. Thresholds, along with previous ramp forecasts, are used to set the ramp signal strength. The ramp signal strength is set to 1 for a weak signal (a low percentage of sites are ramping across relevant groups and times). The signal strength is 2 if a moderate percentage of sites are ramping and set to 3 if a high percentage of sites are ramping across relevant groups and times. The signal strength is set to 4 if the current run's signal strength is at least 2 and a ramp was indicated at the same time slot in the previous three ramp forecasts. Ramp forecasts are created every hour and are delivered via a web page. See Figure 4 for an example of the web display.

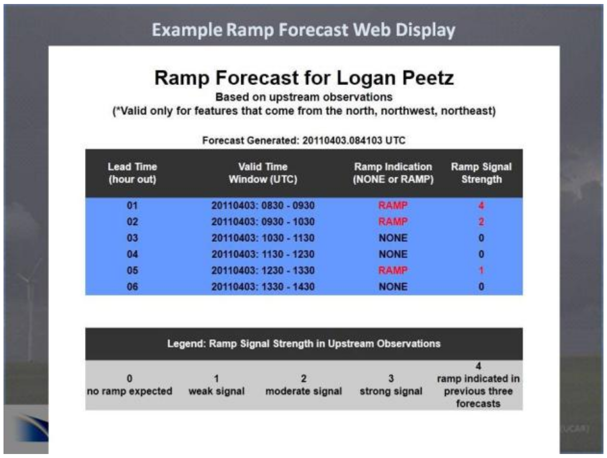

Figure 4. Example ramp forecast web display

4. VERIFICATION

This type of forecast, with either a hit if a ramp actually did occur in the time-window it was forecast or a miss if it did not occur in the time-window it was forecast would normally be a good candidate to use the Critical Success Index (CSI) for verification; But because the prototype was only set up to look for northern originating ramps, CSI statistics could not be calculated accurately because there was no way to tell which direction of propagation of the observed ramp. Therefore numerous case studies were examined to assess the algorithms skill. The verification analysis is based on plots that compare the observation based ramp forecasts to the operational NCAR power forecasts leading up to each event.

The plots show NCAR wind-power node forecasts generated 6 hours, 4 hours and 2 hours before the ramp event (indicated by the colored lines in each plot). The node power forecast is the sum of turbines' power at the farm and is the expected total power at the node. The observed power (indicated by the black line in the plots) was measured directly at the farm node and provided by Xcel Energy. The plots also indicate the observation based ramp forecasts generated 5 hours, 4 hours, 3 hours, 2 hours, and 1 hour before the ramp. The numbers in red represent the signal strength of wind-ramping in upstream observations. Ramp prediction is for a 1-hour window; thus, a ramp indicated at 09z means that a ramp is possible between 09z-10z.

a. Case 1: October 12, 2010

This ramp was caused by a cold front moving in from the north, associated with a strong upper-level storm system moving into the central plains, see Figure 5. Along with the wind, a band of rain and snow moved in behind the front.

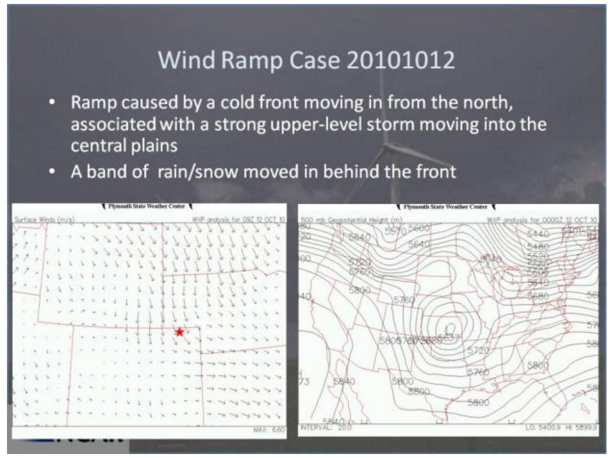

Figure 5. Case 1 weather depiction

Figure 6 shows that the operational power forecasts did well indicating that there would be a large ramp associated with the cold-front but were 2-4 hours too early with the ramp start depending of which forecast you look at. In general the observation-based ramp forecast missed the initial small ramp at around 07z by about 1-2 hours but did very well predicting the main ramp between 10z-11z. By looking at the pattern of ramp forecasts from run to run, it is clear that a significant ramp would occur in the 08z-11z time frame. Overall the ramp forecast did a much better job indicating the start time than did the operational power forecasts.

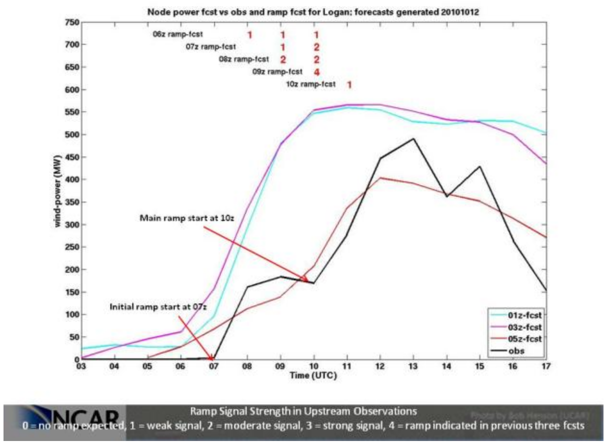

Figure 6. Case 1 verification plot comparing operational power forecasts to observation-based ramp forecasts

b. Case 2: February 8, 2011

The ramp was caused by an arctic cold front moving in from the northeast, associated with a strong upper-level storm system digging into northwestern Colorado, as seen in Figure 7. Strong upslope wind and snow moved in behind the front.

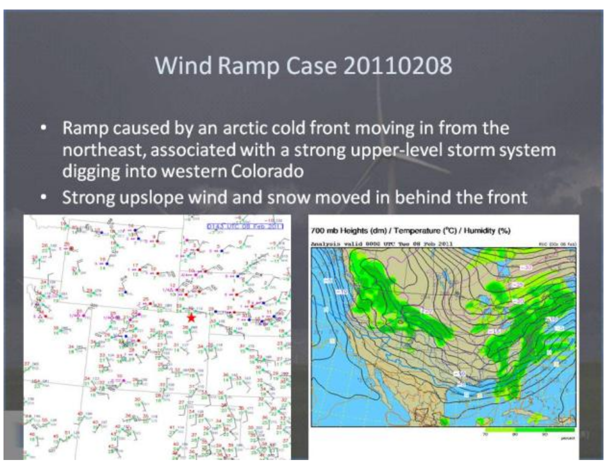

Figure 7. Case 2 weather depiction

Figure 8 shows that all of the operational power forecasts leading up to the event accurately predicted a large ramp but were about 2-3 hours late with the ramp start time. In general, the observation-based ramp forecasts were consistent in showing a significant ramp between 02z-03z. This was about 1 hour late compared to the main ramp start at 01z but was much closer to the onset than the operational power forecasts indicated. Similar to the first case, the pattern in the ramp forecasts gives a good indication about when the ramp event will be centered in time.

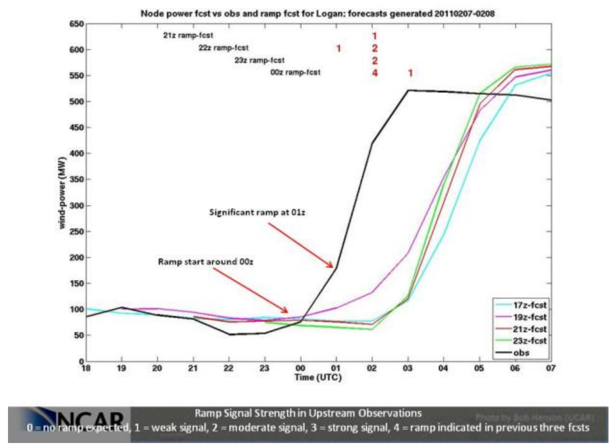

Figure 8. Case 2 verification plot comparing operational power forecasts to observation-based ramp forecasts

c. Case 3: July 11, 2010

For this case there were two ramps that were caused by separate, independent lines of thunderstorms moving over / near the farm. The convection was associated with a summer cold-front and upper-level short-wave moving across northern Colorado, see Figure 9.

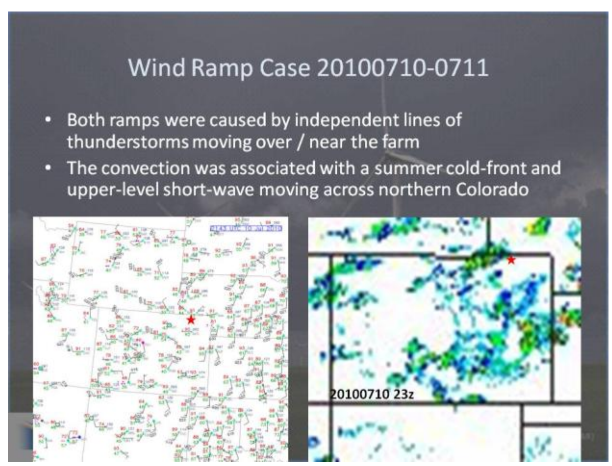

Figure 9. Case 3 weather depiction

Figure 10 shows that all of the operational power forecast leading up to the event missed both ramps. However, the last power forecast, issued between the first ramp and the second, did well at predicting the second ramp (which occurred within the same hour as the forecast was issued). It is not surprising that most of the operational power forecasts missed the ramps since both ramps were caused by isolated thunderstorms moving near the farm, and the model consensus approach typically washes out convective details.

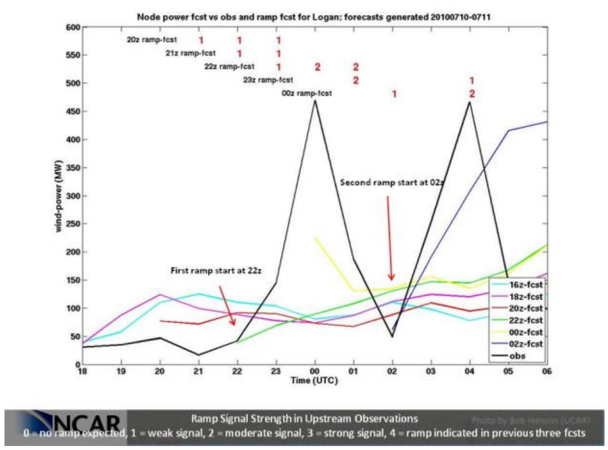

Figure 10. Case 3 verification plot comparing operational power forecasts to observation-based ramp forecasts

The initial observation based ramp forecasts indicated weak ramping for ever hour between 21z-00z. Subsequent ramp forecasts continued to show weak to moderate ramping at different hours from 00z-03z. Although the ramp forecasts predicted ramping near the times the actual ramps occurred (22z-00z and 02z-04z), the pattern and strength in the ramp forecasts were too sporadic to deduce when the big ramps would actual occur. The last two ramp forecasts also showed some additional ramping between 04z-05z and this was two hours late compared to the actual second ramp start at 02z. Overall the ramp forecasts also struggled for this event and this is not surprising since the thunderstorms only moved over some of the sites upstream from the farm.

d. Case 4: February 15, 2011

This ramp was caused by a lee-trough and associated strong jet-stream maxima moving across southern WY (a west to east moving front), see Figure 11. This was a westerly down-slope wind-event with no precipitation.

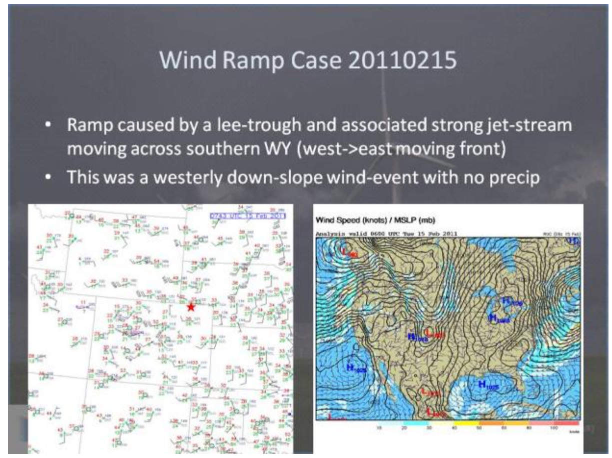

Figure 11. Case 4 weather depiction

Figure 12 shows that the operational power forecast indicated a large ramp would occur for this event but were 2-3 hours early predicting the ramp start time. The observation-based ramp forecasts were consistent, showing initial weak ramping between 08z-09z and a significant ramp between 09z-10z. This was about 1-2 hours later than the actual ramp start time of 07z, but closer to the start than the operational power forecasts indicated. The later ramp forecast, issued at 08z indicated a secondary week ramp between 11z-12z and this was slightly too early compared to the actual second ramp start time at 12z.

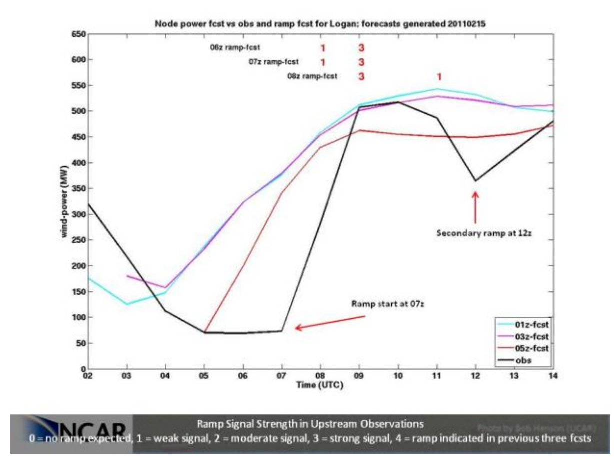

Figure 12. Case 4 verification plot comparing operational power forecasts to observation-based ramp forecasts

e. Case 5: April 3, 2011

The ramp was caused by a northwest originating cold-front associated with a strong surface low moving east / northeast of WY, see Figure 13. This was a dry cold front, with pressure-gradient driven wind.

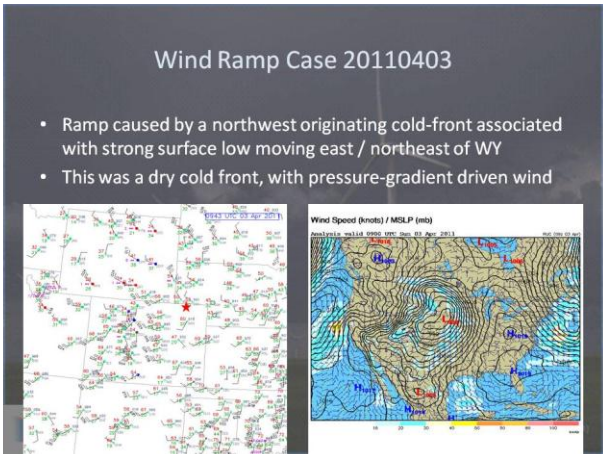

Figure 13. Case 5 weather depiction

Similar to some of the other cold-front cases, Figure 14 shows the operational power forecasts predicted there would be a ramp associated with this event but were off with the timing. The power forecast leading up to the event were consistently 4 hours too late with the onset of the ramp at 10z. The observation based ramp forecasts were consistent showing ramping between 09z-10z and 10z-11z. Although this was slightly early compared to the actual start, overall the ramp forecasts did very well predicting a significant ramp in the 10z-11z time frame and were much better with the timing compared to the operational power forecasts. Weak ramp signals were also predicted to occur between 13z-14z and 14z-15z. These were false-alarms since the actual ramp had leveled out at this point.

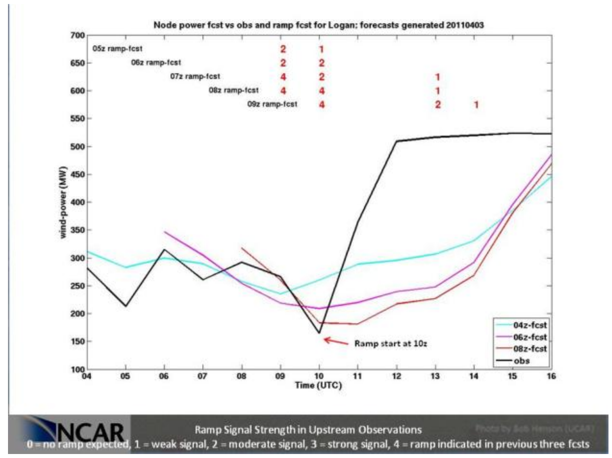

Figure 14. Case 5 verification plot comparing operational power forecasts to observation-based ramp forecasts

f. Case 6: June 26, 2011

For this event, a very large ramp was caused by the combination of convective out-flow and a trailing cold front associated with a surface low tracking east / southeast of Wyoming, see Figure 15. This was a dry front, with strong winds along and immediately behind the front and line of thunderstorms.

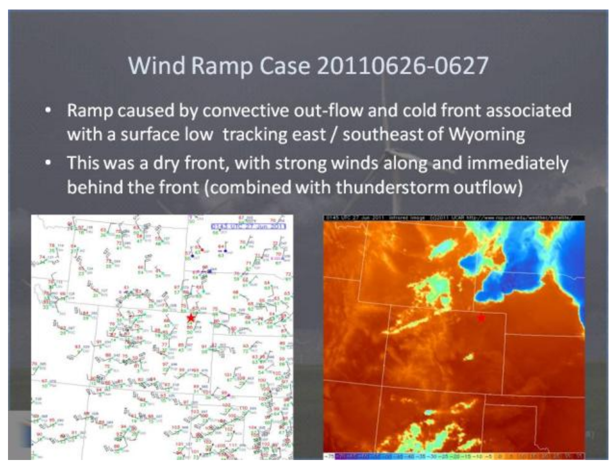

Figure 15. Case 6 weather depiction

Figure 16 shows that all three power forecasts predicted a significant ramp for this event but were consistently about 4-5 hours too early with the ramp start. The power forecasts also underestimated the slope of the power increase, which was extraordinarily sharp due to the combination of convective outflow and a cold front. Most of the observation-based ramp forecasts showed moderate to substantial ramping between 22-23z and 23z-00z compared to the actual ramp start at 01z. The later runs also indicated some continued weak ramping between 00z-01z. The 18z forecast predicted a ramp between 19z-20z and this was a false alarm. Overall, the ramp forecasts did a slightly better job predicting the ramp onset compared to the power forecasts but were still 2-3 hours too early with the ramp start and did not pick up on the strength / timing of the ramp associated with the convective outflow.

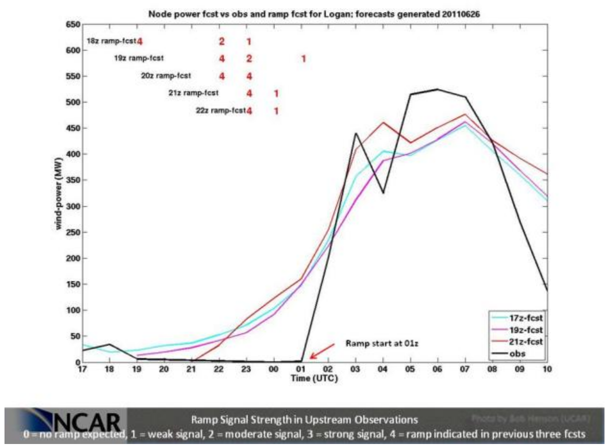

Figure 16. Case 6 verification plot comparing operational power forecasts to observation-based ramp forecasts

5. RESULTS SUMMARY

This study was a proof of concept to show that upstream observations can be used to detect wind features that may cause a power ramp at a wind farm within a 6 hour time frame. The case studies show that the observation-based ramp forecasts do well for synoptic-scale events such as cold-fronts and pressure gradient driven wind events. The observation-based method does not do well predicting ramps associated with convection because thunderstorms are usual isolated in nature and may only pass over a few sites upstream from the farm. The algorithm frequently produces false alarms for “weak-signal = 1”. Since the application was only configured to detect northern originating ramps, CSI (pod, far) stats could not be calculated accurately because there was no way to determine what direction the actual ramp at the farm came from.

Overall, for synoptic events, the observation-based ramp forecast usually gives a better indication of when the ramp is going to occur compared to the operational power forecasts. By combining information from both the operational power forecasts and the observation-based ramp forecast an energy operator could better deduce the timing of a ramp event.

6. FUTURE WORK

The prototype observation-based wind ramp expert system is a proof-of-concept demonstration project; therefore there are many things in the application that could be improved upon. Future improvements that have been proposed include developing a regime-dependent system that is unique to different regions and different types of weather that produce ramps. This includes modifying the algorithm to consider an observing site’s relevance to the prevailing wind-direction. For example if the wind-direction is from the west, one should not include sites that are to the east of the farm as they would no longer be relevant in predicting downstream features. The algorithm could also be easily modified to resolve wind-ramp features coming from all direction, rather than only from the north.

Recently work was done to eliminate some false alarms by only indicating ramps for moderate and strong signals (2’s, 3’s and 4’s) and no longer show weak signals = 1. The algorithm could be modified to predict down-ramps instead of up-ramps by looking for a 25% decrease in pseudo power instead of an increase. The speed of the wind-feature could be dynamically calculated by looking at the distances between sites and the time at which the event occurs at each site.

Finally, the algorithm is at the mercy of the observing site locations and density or lack-there-of. Based on what has been shown in this paper, the application would produce better results if meteorological towers were strategically placed in rings well upstream of the farm, in all directions, rather than just immediately adjacent to the farm.

7. ACKNOWLEDGEMENTS

The author would like to thank the entire NCAR development team that has been part of the Xcel Wind Power project. The author would also like to acknowledge and thank Xcel Energy, as this work would not be possible without their ongoing support.

8. REFERENCES

Myers, W. and S. Linden, 2011: A Turbine Hub Height Wind Speed Consensus Forecasting System. Ninth Conference on Artificial Intelligence and its Applications to the Environmental Sciences, Seattle, WA, Jan 24.